



## Orange-II removal from simulated wastewater by adsorption using *Annona squamosa* shell – A kinetic and equilibrium studies

G.H. Sonawane<sup>a</sup>, V.S. Shrivastava<sup>b\*</sup>

<sup>a</sup>Department of Chemistry, Kisan Arts, Commerce and Science College, Parola, Dist. Jalgaon 425111 (M.S.), India  
Tel.: +912564 234248; email: drvinod\_shrivastava@yahoo.com

<sup>b</sup>Department of P.G. Studies and Research in Chemistry, G.T.P. College, Nandurbar 425412 (M.S.), India

---

### ABSTRACT

Adsorbent prepared from *Annona squamosa* (Custard apple) fruit shell (CAS) were successfully used to remove Orange II from aqueous solution in a batch process. The influence of contact time, initial dye concentration, adsorbent dose and pH has been determined. The optimum contact time and pH for removal of dye was 40 min and 4, respectively. Kinetic parameters of adsorption such as Lagergren pseudo-first order, pseudo-second order, Elovich and intraparticle diffusion model were determined. The experimental data fitted well to the pseudo-second-order kinetic model  $r^2 > 0.9854$  for all concentrations (5–40 mg/L) tested. Both Freundlich and Langmuir isotherms could be used to describe the adsorption dye, with the former yielding somewhat better fits. In addition, adsorbent was characterized by FTIR, XRD and SEM analysis.

**Keywords:** *Annona squamosa*; Orange II; Colour removal; Adsorption Isotherms; Kinetics; Batch study

---

### 1. Introduction

Many industries such as textile, leather tanning, food, paper and pulp consumes dyes extensively. Among them textile industry ranks first in the usage of dyes for coloration of fiber [1]. The generated colored effluents containing various dyes and pigments and discharge the same to natural water bodies. Such effluents are characterized by fluctuating pH with large load of suspended solids and high oxygen demand [2]. These wastewaters cause many damages to the ecological system of the receiving surface water [3].

Dyes are a kind of organic compounds with a complex aromatic molecular structure that can bring bright and firm color to other substances. However, the

complex aromatic molecular structures of dyes make them more stable and difficult to biodegrade [4]. Many dyes and pigments are toxic and have carcinogenic and mutagenic effects [5] that effect aquatic biota and also humans [6]. Due to the chemical stability of the dye components, conventional wastewater treatment technologies are often ineffective for handling wastewater containing synthetic textile dyes [7].

Considerable efforts have been made by many researchers to find appropriate treatment systems in order to remove pollutants and impurities of wastewater from textile industry [8]. Many chemical and physical methods of dye removal including photocatalytic degradation [9], membranes [10] and adsorption techniques [11,12] have been used from time to time. Adsorption process is noted to be superior to other removal techniques because it is economically cost effective, simple and it is capable to efficiently treat

---

\*Corresponding author

dyes in more concentrated form [13]. Activated carbon is popular and an effective dye adsorbent, but its relatively high price, high operating costs and problems with regeneration hamper its large scale applications. Therefore, there is a growing need in finding low cost, renewable, locally available materials as adsorbent for the removal of dye colors [14,15].

The *Annona squamosa* (Custard apple) of family Annonaceae is native to the India sub-continent. Its seeds, shell and leaves have been in use since ancient times to treat number of human ailments and also as a household pesticide [16]. Custard apple shell (CAS) is a fruit waste material. After removal of fruit pulp from ripened fruits, the shells are discarded; such waste shell material is available at no or low cost which is used as adsorbent.

The purpose of this study was to evaluate the suitability of *Annona squamosa* shell (CAS) for adsorption of Orange II dye.

## 2. Materials and methods

### 2.1. Adsorbent material

The ripened custard apple fruits were collected from local market, after removal of fruit pulp, shells are separated. The collected shell material was washed with tap water and dried in sunlight and powdered using still mill. The adsorbent was then sieved to 80–100 mesh, soaked in water for 12 h and washed with cold and hot distilled water till the washed water is colorless. The washed material was then dried in hot air oven at 50°C for 12 h and preserved in desiccators for further used as CAS adsorbent.

### 2.2. Preparation of simulated dye waste water

The dye, Orange II was synthesized in laboratory and purified [17]. The dye stock solution of 2,000 mg/L was made by dissolving required amount of the dye in double distilled water. The experimental solutions were obtained by diluting the dye stock solution to needed initial concentrations. The initial pH of each dye solution was adjusted with 0.1 M NaOH or HCl using pH meter to its effective adsorption pH value obtained from the results of earlier experiments.

### 2.3. Method

The adsorption experiments were carried out in a batch process at 30°C by shaking adsorbent with 50 cm<sup>3</sup> dye solution of required concentration and pH. The sample was withdrawn from the shaker and dye solution was separated from adsorbent by centrifugation. Dye concentration in the supernatant solution

was estimated by measuring absorbance at maximum wavelength ( $\lambda_{\max} = 580$  nm) and computing concentration from calibration curve. Kinetics of adsorption was determined by analyzing adsorptive uptake of dye from aqueous solution at different time intervals. Isothermal studies were conducted by adding various doses of adsorbent and shaking the reaction mixture for equilibrium time. The residual color for equilibrium contact times was then determined.

The FTIR, elemental analysis, scanning electron microscopy (SEM) and X-ray diffraction (XRD) of CAS adsorbent was also carried out.

## 3. Results and discussion

### 3.1. FTIR and elemental analysis

The FTIR measurement of MCP showed the presence of peaks for large number of functional groups viz., 3334.7 –OH stretching, 2891.1 C–CH<sub>3</sub> alkane stretching, 1735 –C– stretching, 1600.8 aromatic –C=C–, 1427.2 –C–H, –CH<sub>2</sub>, –CH<sub>3</sub>, deformations 1369.4 –O–C–CH sharp band, 1326.9 –O–H bending, 1238.2 –C–O– stretching frequency in ester, 1051.1 primary –OH, 894.9 R<sub>2</sub>C=CH<sub>2</sub>, 827.4 R<sub>2</sub>C=CHR. It contains large number of polar groups on the surface which is likely to give considerable dye adsorption capacity to CAS.

The elemental analysis of CAS show C = 63.97%, O = 30.61%, H = 2.19, Na = 0.13%, Al = 0.05%, P = 0.68%, S = 1.74% and Ca = 0.63%.

### 3.2. SEM analysis

Scanning electron microscopy (SEM) is widely used to study the morphological features and surface characteristics of adsorbent materials. The CAS and CAS dyed by Orange II were analyzed by SEM (Fig. 1). It shows surface texture and porosity of CAS. The CAS has heterogeneous surface, micro pores as seen from its surface micrographs. Its Braunauer-Emmett-Teller (BET) surface area confirms that CAS has micropores and mesopores.

Textural characterization of the CAS was carried out by N<sub>2(g)</sub> adsorption at 77 K using ASAP 2010 micro pore analyzer. The BET surface area, pore volume and pore diameter were then determined. The BET surface area was found to be 11.32 m<sup>2</sup>/g Langmuir surface area 24.62 m<sup>2</sup>/g micro pore area 0.72 m<sup>2</sup>/g, mesopore area 242.63 m<sup>2</sup>/g, micro pore volume 0.0012 cm<sup>3</sup>/g, mesopore volume 23.06 cm<sup>3</sup>/g, mean pore diameter 8.32 Å and mean mesopore diameter 363.81 Å.

### 3.3. XRD analysis

The XRD diagram of CAS has been shown in Fig. 2. The XRD pattern of adsorbent shows typical spectrum

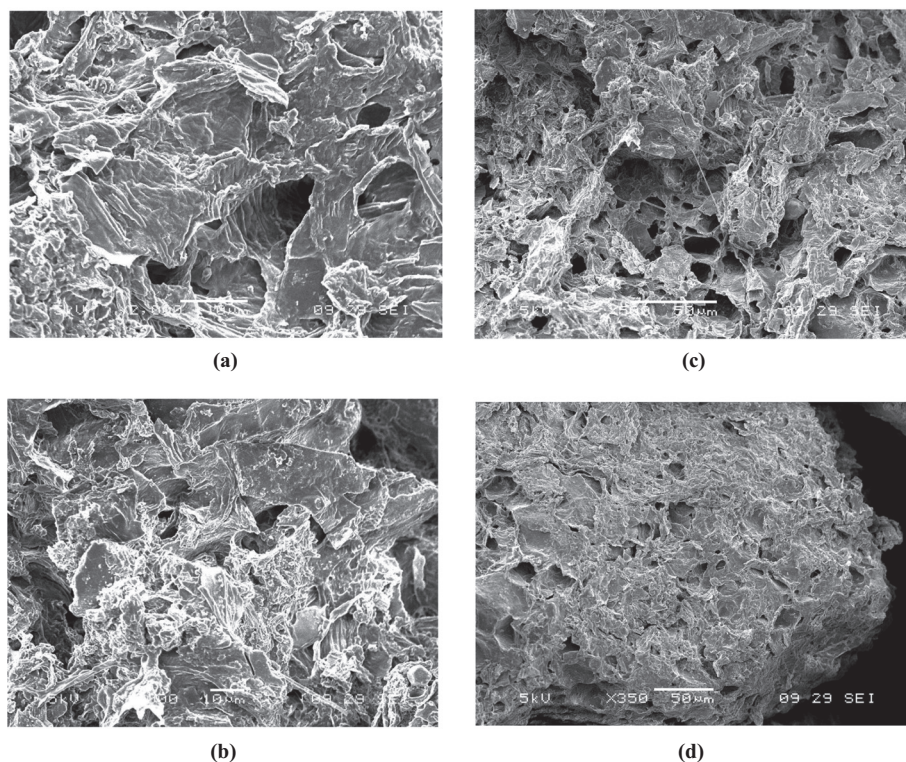


Fig. 1. The SEM micrographs of CAS and CAS dyed by Orange II.

of cellulosic material. It shows main and secondary peaks at  $2\theta$  of  $22^\circ$  and  $42^\circ$ , respectively.

#### 3.4. Effect of pH

The pH of the solution is an important process controlling parameter in the dye adsorption process. The pH will have significant influence on dye adsorption. Adsorption of acid dye exhibits different behavior than basic dye. For Orange II an acid dye, adsorption was found to decrease with increasing with  $H^+$ . Higher pH will produce more  $OH^-$  ions in solution, preventing the adsorption of dye anions on the adsorbent surface. Similar behavior has also been reported by other researchers [18].

The effect of pH on removal of Orange II using 20 mg/L of dye and 8 g/L of adsorbent dose was studied. As pH increased from 2 to 4, the percent removal also increases from 73.3% to 85.3%. When pH was further increased up to 10, percent removal decreases to 76.1%. Hence significant adsorption of Orange II on CAS was observed at pH 4. The observed low adsorption of Orange II on CAS at  $pH < 4$  may be because of the surface charge becomes negatively charged, thus making ( $H^+$  ions) compete effectively with dye anions causing a decrease in the amount of dye adsorbed.

At pH 4 a considerable high electrostatic attraction exist between positively charged surface of the adsorbent, due to the ionization of functional groups of adsorbent and negatively charged anionic dye molecules. Also lower adsorption of Orange II dye at alkaline pH is due to presence of excess of  $OH^-$  ions destabilizing anionic dyes and competing with dye anions for adsorption sites. Thus effective pH was 4 and it was used in further studies.

#### 3.5. Effect of contact time and dye concentration

Fig. 3 shows the effect of dye concentration and agitation time on dye removal. The equilibrium time was found to be 40 min. The amount of dye adsorbed per unit weight of adsorbent increased from 0.4637 to 2.2651 mg dye/g of adsorbent when initial dye concentration was increased from 5 to 30 mg/L (Fig. 4). As other variables such as adsorbent dosage, pH and agitation speed were same for different experimental runs, the dye concentration affected the diffusion of dye molecules through the solution to the surface of the adsorbent. Higher concentration resulted in higher driving force of the concentration gradient. This driving force accelerated the diffusion of dye from solution into the adsorbent [19]. It is clear that the efficiency of dye

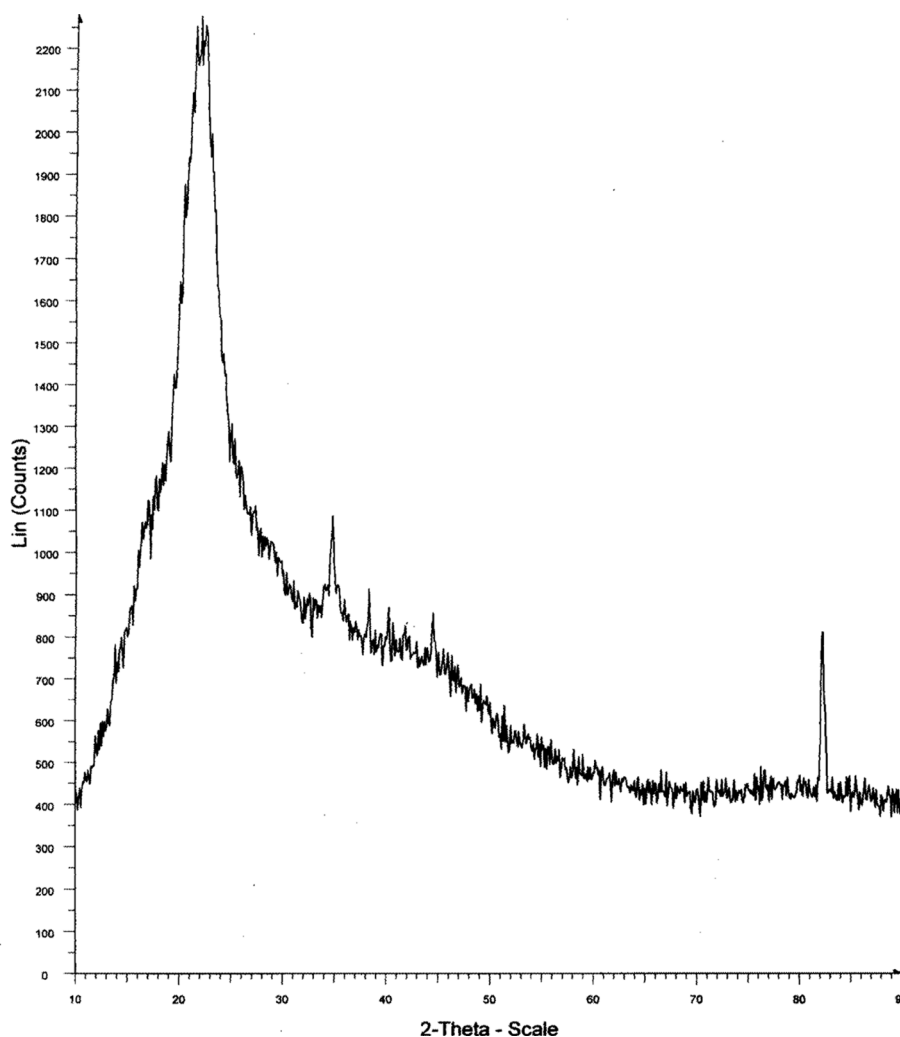


Fig. 2. The XRD diagram of CAS adsorbent.

removal depends on the initial dye concentration. The amount of dye adsorbed increased with increase in dye concentration and remained nearly constant after the equilibrium time.

### 3.6. Effect of adsorbent dosage

Fig. 5 shows the removal of Orange II by CAS at different adsorbent doses (2–21 g/L) for the dye concentrations 10, 20, 30 and 40 g/L. As adsorbent dose increases the percent removal of dye also increases, which is due to the increase in adsorbent surface area and availability of more adsorption sites. But unit adsorption was decreased from 4.924 to 0.8555 mg/g as adsorbent dose was increased from 2 to 21 g/L. This may be attributed due to overlapping or aggregation of adsorption sites resulting in decrease in total adsorption sites resulting in decrease in total

adsorbent surface area available to Orange II and increase in diffusion path length.

### 3.7. Adsorption kinetics

Kinetics of adsorption is quite significant as it decides residence time of adsorbate at the rate of the adsorption process. The kinetics of adsorption of Orange II on CAS was analyzed with the help of pseudo-first order, pseudo-second order, Elovich and intraparticle diffusion models.

#### 3.7.1. The pseudo-first-order equation.

The Lagergren pseudo-first-order equation has been widely used to predict dye adsorption kinetics. A linear plot of  $\log(q_e - q_t)$  vs.  $t$  verifies the first-order kinetics with the slope yielding the value of the

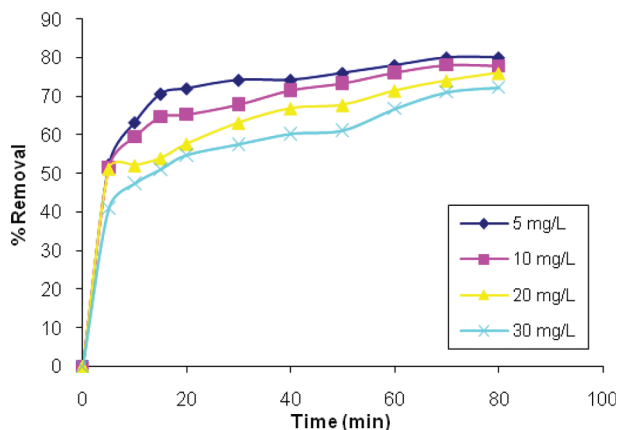


Fig. 3. Effect of contact time and concentration of Orange (II) on percent removal; adsorbent dose 8 g/L, pH 4.

rate constant. A linear form of pseudo-first-order model was described by Lagergren [20].

$$\log(q_e - q_t) = \log q_e - \frac{K_1 t}{2.303} \quad (1)$$

where  $q_e$  and  $q_t$  are the amount of dye adsorbed per unit mass of adsorbent ( $\text{mg g}^{-1}$ ) at equilibrium and at time  $t$ , respectively.  $K_1$  is pseudo-first-order rate constant ( $\text{min}^{-1}$ ). The linear relationship of the plot of 5, 10, 20 and 30 mg/L dye concentration indicates the validity of equation. Even though, the correlation coefficients  $r^2$  for the plots were in the range of 0.9742–0.9936, which are considerably high. The first-order rate constants evaluated from these plots were between  $5.13 \times 10^{-2}$  to  $13.21 \times 10^{-2} \text{ min}^{-1}$  for different amount of adsorbents. The dye-CAS interactions could thus be predicted reasonably fast. In the present work  $q_e$  values calculated from first-order kinetic plots were for too

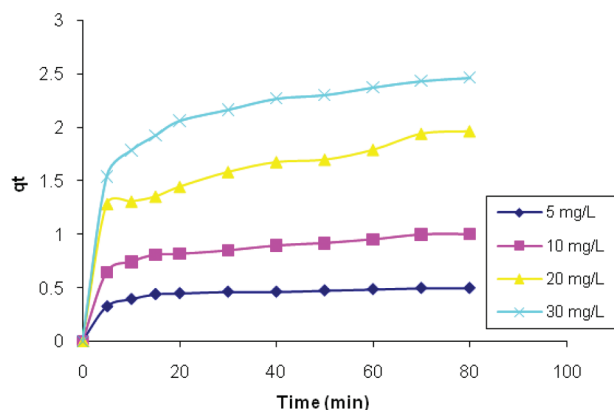


Fig. 4. Amount of dye adsorbed  $q_t$  ( $\text{mg/g}$ ) with time for different initial dye concentration; adsorbent dose 8 g/L pH 4.

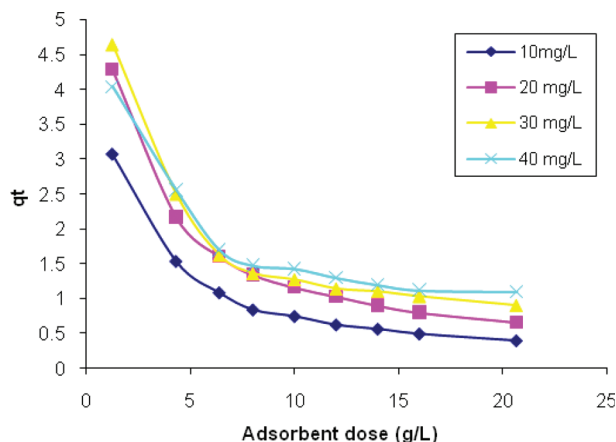


Fig. 5. Amount of dye adsorbed ( $\text{mg/g}$ ) with adsorbent dose for different initial dye concentrations, contact time 40 min, pH 4.

small compared to the experimental values (Table 1). The Lagergren first-order equation is inapplicable to describe the adsorption kinetics of Orange II was observed from these values.

### 3.7.2. The second-order kinetics equation

The pseudo-second-order kinetic model is expressed as [21].

$$\frac{t}{q_t} = \frac{1}{K_2 q_e^2} + \frac{t}{q_e} \quad \text{and} \quad h = K_2 q_e^2 \quad (2)$$

$K_2$  is the rate constant of second-order adsorption ( $\text{g mg}^{-1} \text{ min}^{-1}$ ). The plot of  $t/q_t$  vs.  $t$  of above equation gives linear relationship (Fig. 6), from which  $q_e$  and  $K_2$  can be determined from slope and intercept of the plot, respectively. The linear plot of  $t/q_t$  vs.  $t$  shows a good agreement of experimental data with the second-order kinetic model for different initial dye concentrations of 5, 10, 20, 30 mg/L. The correlation coefficients ( $r^2$ ) for the second-order kinetic model are greater than 0.9854 (Table 1). The calculated  $q_e$  values agree with the experimental data which indicates that adsorption system belongs to the second-order kinetic model. It is predominant, and the overall rate of the dye adsorption process appears to be controlled by chemisorption process [22,23]. Similar phenomenon has been observed in the adsorption of direct dyes onto activated carbon prepared for sawdust [24,25]. For the pseudo-second-order model, the rate constant decreased with an increase in initial dye concentration and rate constant increases with increase in adsorbent dose.

Table 1

Comparison of adsorption rate constants, calculated and experimental  $q_e$  values for different initial dye concentrations and adsorbent dose for different kinetic models

Adsorbent (g/L)	Concentration (mg/L)	Pseudo first order			
		$q_e(\text{exp})$ (mg/g)	$K_1 \times 10^{-2}$ ( $\text{min}^{-1}$ )	$q_e(\text{cal})$ (mg/g)	$r^2$
8	5	0.4637	13.219	0.2365	0.9792
	10	0.8937	6.609	0.3102	0.9817
	20	1.6712	5.826	0.5691	0.9742
	30	2.2651	7.692	1.0977	0.9919
12	5	0.3416	6.425	0.0585	0.9938
	10	0.6883	5.135	0.1273	0.9935
	20	1.3291	5.319	0.2113	0.9952
16	5	0.2693	6.379	0.0563	0.9874
	10	0.5275	7.461	0.1204	0.9878
	20	1.0025	8.031	0.1712	0.9937
Pseudo Second Order					
		$K_2$ (g/mg/min)	$q_e(\text{cal})$ (mg/g)	$h$	$R^2$
8	5	0.6111	0.5155	0.1624	0.9993
	10	0.1892	1.0439	0.2062	0.9965
	20	0.0665	2.0618	0.2829	0.9898
	30	0.0417	2.9171	0.3550	0.9854
12	5	1.1034	0.3484	0.1580	0.9993
	10	0.5587	0.7375	0.3039	0.9995
	20	0.2512	1.4536	0.5308	0.9987
16	5	1.8625	0.2816	0.1477	0.9918
	10	0.8747	0.5530	0.2675	0.9997
	20	0.3391	1.1150	0.4216	0.9986
Elovich mModel					
		$\beta$ (g/mg)	$r^2$	Intraparticle diffusion $K_p$ (mg/g/min <sup>0.5</sup> )	$r^2$
8	5	17.8891	0.7179	0.0253	0.9241
	10	8.1234	0.9812	0.0497	0.9628
	20	3.8109	0.9076	0.1006	0.9769
	30	2.4051	0.9813	0.1236	0.9552
12	5	37.1744	0.9487	0.0108	0.9656
	10	19.1204	0.9809	0.0288	0.9727
	20	10.4712	0.9608	0.0406	0.9839
16	5	56.8188	0.9742	0.0069	0.9451
	10	30.1204	0.9702	0.0131	0.9418
	20	13.0039	0.9567	0.0308	0.9669

### 3.7.3. The Elovich equation

The dye adsorption fits the Elovich model, the simplified Elovich equation is

$$q_t = l_n(ab) + l_n t \quad (3)$$

where ' $\alpha$ ' is the initial adsorption rate ( $\text{mg g}^{-1} \text{min}^{-1}$ ),  $\beta$  is the desorption constant (g/mg), were calculated from intercept and slope of the straight line plot of  $q_t$  vs.  $\ln t$ . It will be seen from the data that the value of  $\alpha$  and  $\beta$  varied as a function of initial dye concentration. Thus on increasing initial dye concentration from 5 to 30 mg/L, the value of  $\beta$  decreases from 17.889 to

2.405 for 8 g/L of adsorbent dose. The value of  $\beta$  increases from 17.889 to 56.818 as adsorbent dose was increased from 8 to 16 g/L for 5 mg/L of dye solution (Table 2).

### 3.7.4. The intra-particle diffusion model

An empirically found functional relationship, common to most adsorption process, is that the uptake varies almost proportionally with  $t^{1/2}$ , the Weber-Morris plot, rather than with the contact time [26].

$$q_t = K_p t^{1/2} + C \quad (4)$$



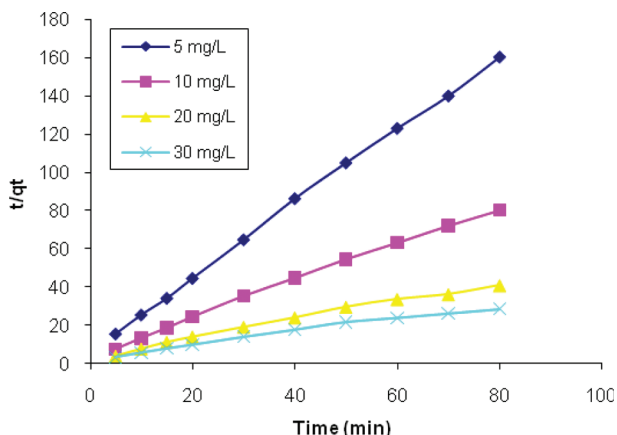


Fig. 6. Second-order kinetic plots for the removal of Orange II at different initial dye concentrations; adsorbent dose 8 g/L, pH 4.

where  $K_p$  is intra-particle diffusion rate constant ( $\text{mg g}^{-1} \text{min}^{-0.5}$ ). According to a plot of  $q_t$  vs  $t^{1/2}$  should be straight line with a slope  $K_p$  and intercept  $C$ . When adsorption mechanism follows the intra-particle diffusion process, values of the intercept give an idea about the thickness of boundary layer effect [27]. The linear plots of  $q_t$  vs  $t^{1/2}$  for Orange II are attributed to the macro pore diffusion, which are the accessible sites of adsorption. This is attributed to the instantaneous utilization of the most readily available adsorbing sites on the adsorbent surface. The values of  $K_p$  as obtained from the slope of straight lines are listed in Table 1.

### 3.8. Adsorption isotherms

Adsorption isotherm are important for the description of how molecules of adsorb ate interact with adsorbent surface and also, are critical in optimizing the use of CAS as an adsorbent. Two well-known isotherm equations the Langmuir and Freundlich have been applied for deeper interpretation of the adsorption data obtained.

#### 3.8.1. Freundlich isotherm

The Freundlich model is applied to describe heterogeneous system characterized by heterogeneity factor of  $1/n$ . The linear plot of  $\log q_e$  vs  $\log C_e$  confirms the applicability of a model. The logarithmic form of Freundlich isotherm equation is

$$\log q_e = \log K_f + \frac{1}{n} \log C_e \quad (5)$$

Where  $q_e$  is the amount of adsorbate absorbed per unit mass of adsorbent ( $\text{mg/g}$ ),  $C_e$  is an equilibrium concentration of dye ( $\text{mg/L}$ ),  $K_f$  is a quantity of dye adsorbed in  $\text{mg/g}$ , adsorbent for unit concentration of dye and  $1/n$  is a measure of adsorption density. Linear plots of  $\log q_e$  vs  $\log C_e$  for 5, 10, 20, 30  $\text{mg/L}$  dye concentration (Fig. 7) shows that the adsorption also follows the Freundlich isotherm. The  $K_f$  and  $n$  values were calculated from intercept and slope of the plots and represented in Table 2. The correlated coefficients in the graph  $r^2 > 0.9699$ , indicates the validity of isotherm.

#### 3.8.2. Langmuir isotherm

Langmuir isotherm is represented by the following equation [28].

$$(C_e/q_e) = (1/ab) + (C_e/b) \quad (6)$$

$C_e$  is the concentration of dye solution ( $\text{mg/L}$ ) at equilibrium. The constant ' $a$ ' signifies the adsorption capacity ( $\text{mg/g}$ ) and ' $b$ ' is related to the energy of adsorption ( $\text{L/mg}$ ). The linear plot of  $C_e/q_e$  vs.  $C_e$  shows that adsorption follows Langmuir isotherm (Fig. 8). Values of ' $a$ ' and ' $b$ ' were calculated from the slope and intercept of the linear plots and are presented in Table 2. The applicability of the Langmuir isotherm suggests the monolayer coverage of the dye on the surface of CAP. The essential characteristics of the Langmuir isotherm can be expressed by dimensionless constant called equilibrium parameter,  $R_L$  [29].

Table 2

Freundlich and Langmuir coefficients for adsorption of Orange II on CAS for different dye concentration and adsorbent dose of 2–21 g/L at pH = 4, contact time 40 min

Dye concentration (mg/L)	Freundlich coefficient				Langmuir coefficient			
	$K_f$ (L/g)	$n$	$1/n$	$r^2$	$a$ (mg/g)	$b$ (g/L)	$R_L$	$r^2$
10	0.1017	0.5063	0.9751	0.9865	0.9236	0.1636	0.3793	0.9623
20	0.2746	0.4974	2.0101	0.9699	1.7041	0.0601	0.4544	0.9518
30	0.3082	0.6420	0.6090	0.9762	2.6096	0.0271	0.5511	0.9172
40	0.4392	2.7525	0.3633	0.9744	2.1486	0.0267	0.4835	0.9631

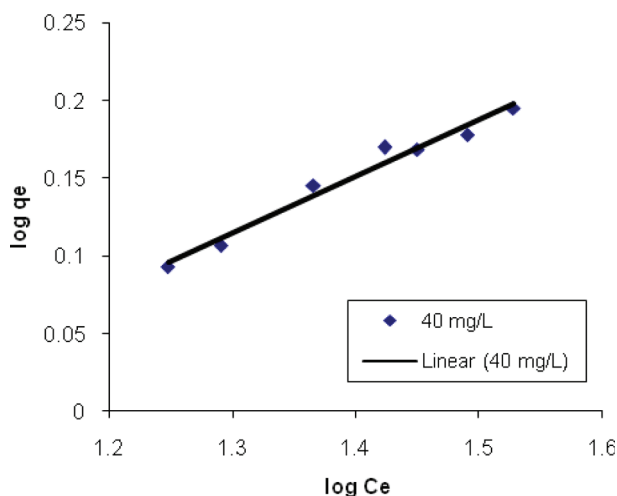


Fig. 7. Freundlich plot for adsorption of Orange II by CAS.

$$R_L = 1/(1 + bC_i) \quad (7)$$

where 'b' is the Langmuir constant and  $C_i$  is the initial dye concentration (mg/L) and  $R_L$  values indicate the type of isotherm, if  $R_L > 1$  unfavorable,  $R_L = 1$  Linear,  $1 > R_L > 0$  favorable and  $R_L = 0$  irreversible adsorption. The calculated values of  $R_L$  are presented in Table 2, shows that  $R_L$  values between zero and one which confirm the favorable uptake of Orange II.

The Freundlich and Langmuir coefficients are shown in Table 2, both the isotherms were found to fit well to the experimental data, with the former being slightly better as indicated by the higher  $r^2$  values.

#### 4. Conclusion

In the laboratory scale studies conducted, CAS was capable of adsorbing Orange II from aqueous solutions. The adsorption capacity was found to be affected

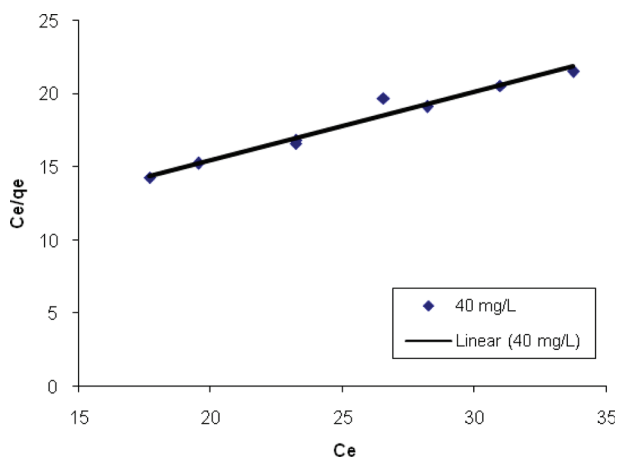


Fig. 8. Langmuir plot for adsorption of Orange II by CAS.

by solution pH, with lower pH 4 favoring adsorption. The amount of dye adsorbed increased with the increase in contact time and initial dye concentrations. The equilibrium time was 40 min. Adsorption of dye could be described by both the Freundlich and Langmuir isotherms, the former yielding somewhat better fits. The dimensionless separation factor  $R_L$  called as equilibrium parameter showed that CAS can be used for removal of Orange II from aqueous solution. The adsorption kinetics followed the pseudo second order model indicating the chemisorptions were rate controlled step in the adsorption of Orange II.

Thus CAS is an inexpensive and easily available fruit waste material that can be used as alternative of more costly adsorbent used for dye removal in wastewater treatment process.

#### Acknowledgments

The authors are gratefully acknowledged to the Head, Centre for Nonmaterial and Quantum Systems, Department of Physics, University of Pune for Scan Electron Microscopy and XRD analysis. Authors are also thankful to Principal, GTP College Nandurbar for providing necessary laboratory facilities.

#### References

- [1] V.K. Garg, R. Gupta, A.B. Yadav and R. Kumar, Dye removal from aqueous solution by adsorption on treated sawdust, *Biores. Technol.*, 89 (2003) 121–124.
- [2] R. Sivraj, C. Namasivayam and K. Kadirvelu, Orange peel as an adsorbent in the removal of Acid Violet 17 (acid dye) from aqueous solution, *Waste Manag.*, 21 (2001) 105–110.
- [3] F.D. Ardejani, K. Badii, N.Y. Limaee, N.M. Mahmoodi and A.R. Mirhabibi, Numerical modeling and laboratory studies on the removal of Direct red-23 and Direct red-80 dyes from textile effluents using orange peel, a low cost adsorbent, *Dyes Pig.*, 73 (2007) 178–185.
- [4] A. Reife and H.S. Freeman, Pollution prevention in the production of dyes and pigments, *Textile Chemistry of Color*, American Dyestuffs Report, 32 (2000) 56–60.
- [5] P.K. Dutta, An overview of textile pollution and its remedy, *Ind. J. Environ. Protect.*, 14 (1994) 443–446.
- [6] A.R. Gregory, S. Elliot and P. Kluge, Ames testing of Direct black 3B parallel carcinogenicity, *J. Appl. Toxicol.*, 1 (1991) 308–313.
- [7] E. Forgacs, T. Cserhati and G. Oros, Removal of synthetic dyes from wastewater: a review, *Environ. Int.*, 30 (2004) 953–971.
- [8] D. Georgion, P. Melidis, A. Aivasidis and K. Gimouho-poulos, Degradation of azo reactive dyes by ultraviolet radiation in the presence of hydrogen peroxide, *Dyes Pig.*, 52 (2002) 69–78.
- [9] L.S. Tsui, W.R. Roy and M.A. Cole, Removal of dissolved textile dyes from wastewater by a compost sorbent, *Color. Technol.*, 119 (2003) 14–18.
- [10] J. Wu, M.A. Eiteman and S.E. Law, Evaluation of membrane filtration and ozonation process for treatment of reactive dye wastewater, *J. Environ. Eng.*, 124 (1998) 272–277.
- [11] G. Annadurai, R.S. Juang and D.J. Lee, Factorial design analysis for adsorption of dye on activated carbon beads incorporated with calcium alginate, *Adv. Environ. Res.*, 6 (2002) 191–198.



- [12] D. Mohan, K.P. Sinigh, G. Singh and K. Kumar, Removal of dyes from wastewater using fly ash, a low cost adsorbent, *Ind. Eng. Chem. Res.*, 41 (15) (2002) 3680–3695.
- [13] C. Hachem, F. Bocquillon, O. Zehraa and M. Bouchy, Decolorization of textile industry wastewater by the photo catalytic degradation process, *Dyes Pig.*, 49 (2001) 117–125.
- [14] K.V. Kumar, V. Ramamurthi and S. Sivanesan, Modeling the mechanism involved during the sorption of methylene blue onto fly ash, *J. Coll. Int. Sci.*, 284 (2005) 14–21.
- [15] S.B. Wang, Y. Bayjoo, A. Chueib and Z.H. Zhu, Removal of dyes from aqueous solution using fly ash and red mud, *Water Res.*, 39 (2005) 129–138.
- [16] P. Shukla and S.P. Misra, *An Introduction in Taxonomy of Angiosperms*, Vikas Publication, pp. 223–227.
- [17] B.S. Furniss, A.I. Hanneford, P.W.G. Smith and A.K. Tatchell, *Vogel's Textbook of Practical Organic Chemistry*, Pearson Education, 5th ed., 2007, pp. 950–951.
- [18] D. Mohan, K.P. Singh, G. Singh and K. Kumar, Removal of dyes from wastewater using fly ash, a low cost adsorbent, *Ind. Eng. Chem. Res.*, 41 (2002) 3688–3695.
- [19] M. Ozocar and A.I. Sengil, Adsorption of metal complex dyes from aqueous solutions by pine sawdust, *Biores. Technol.*, 96 (2005) 791–795.
- [20] Z. Aksu and S. Tezer, Equilibrium and kinetic modeling of biosorption of removal black B by rhizopus anhisus in a batch system – effect of temperature, *Process Biochem.*, 36 (2000) 431–439.
- [21] V.V. Goud, K. Mohanty, M.S. Rao and N.S. Jaykumar, Phenol removal from aqueous solutions by tamarind nutshell activated carbon: batch and column studied, *Chem. Eng. Technol.*, 7 (2005) 28–29.
- [22] G. McKay and Y.S. Ho, The sorption of lead (II) on peat, *Water Res.*, 33 (1999) 578–584.
- [23] G. McKay and Y.S. Ho, Pseudo-second order model for sorption processes, *Process Biochem.*, 34 (1999) 451–465.
- [24] P.K. Malik, Dye removal from wastewater using activated carbon developed from sawdust: adsorption equilibrium and kinetics, *J. Hazard. Mater.*, B113 (2004) 81–88.
- [25] C. Namasivayam and D. Kavitha, Removal of Congo red from water by adsorption onto activated carbon prepared from coir pith, an agricultural solid waste, *Dyes Pig.*, 54 (2002) 47–58.
- [26] Weber and J.C. Morris, Kinetics of adsorption on carbon from solution, *J. Sanit. Eng. Div., Am. Soc. Civil Eng.* (1963) 89–31.
- [27] K. Kannan and M.M. Sundaram, Kinetics and mechanism of removal of methylene blue by adsorption on various carbons – a comparative study, *Dyes Pig.*, 51 (2001) 25.
- [28] I. Langmuir, The adsorption of gases on plane surfaces of glass, mica and platinum, *J. Am. Chem. Soc.*, 40 (1918) 1361.
- [29] W. Shaobin and L. Huiting, Kinetic modeling and mechanism of dye adsorption on unburned carbon, *Dyes Pig.*, 72 (2007) 308–314.